Journal for ImmunoTherapy of Cancer

Therapeutic vaccination for glioblastoma elicited by retargeted oncolytic herpes virus

Francesca Piaggio [1], Chiara Riviera [1], Francesco Alessandrini [2], Daniela Marubbi [1,2], Davide Ceresa [2], Irene Appolloni [1,2], Agnese Vincenzi [1], Tatiana Gianni [3], Gabriella Campadelli-Fiume [3], Paolo Malatesta [1,2]

To cite: Piaggio F, Riviera C, Alessandrini F, *et al*. Therapeutic vaccination for glioblastoma elicited by retargeted oncolytic herpes virus. *Journal for ImmunoTherapy of Cancer* 2026;**14**:e012840. doi:10.1136/jitc-2025-012840

► Additional supplemental material is published online only. To view, please visit the journal online (https://doi.org/10.1136/jitc-2025-012840).

Accepted 19 December 2025

[1]IRCCS Ospedale Policlinico San Martino, Genoa, Italy
[2]Dipartimento di Medicina Sperimentale, University of Genoa, Genoa, Italy
[3]Department of Medical and Surgical Sciences, University of Bologna, Bologna, Italy

Correspondence to
Dr Francesca Piaggio;
francesca.piaggio@aomliguria.it

Dr Paolo Malatesta;
paolo.malatesta@unige.it

Tatiana Gianni;
tatiana.gianni3@unibo.it

ABSTRACT

Background Glioblastoma is an aggressive tumor with poor prognosis and limited treatment options due to its resistance to chemotherapy and radiotherapy, high heterogeneity, and ability to evade the immune system. Nevertheless, immunotherapy and oncolytic virotherapy are emerging as promising strategies. This study aimed to evaluate the therapeutic efficacy of an engineered oncolytic Herpes Simplex Virus for glioblastoma treatment.

Methods We investigated the efficacy of R-115, a retargeted oncolytic Herpes Simplex Virus directed against the human epidermal growth factor receptor 2 (HER2) and engineered to express murine interleukin-12, in an immunocompetent glioblastoma model that recapitulates HER2 tumor heterogeneity. We tested the translatability and reliability of R-115 by assessing overall survival in $HER2^+$ or $HER2^+/HER2^-$ mixed tumors treated with different schedules. We assessed the potential of the treatment to elicit an antitumor vaccination effect by rechallenging previously treated mice with HER2-negative cells in the absence of any further therapy. Additionally, we characterized both the immune and tumor components by analyzing immune cells' proliferation, activation and the resulting tumor cells reduction.

Results R-115 exhibited potent cytotoxic and immune-stimulatory effects, significantly prolonging survival and eradicating tumors in approximately 25% of treated mice independently from tumor composition and treatment schedule. Furthermore, it induced long-term immune memory, enabling the eradication of secondary transplanted tumors, effectively acting as a tumor-agnostic vaccination. Notably, in addition to the direct oncolysis mediated by the virus, R-115 treatment induced an immune response even against HER2-negative glioblastoma cells, potentially via cross-presentation or epitope spreading.

Conclusions Our findings candidate R-115 as a promising alternative to standard glioblastoma treatments and support further investigation to advance its clinical application.

WHAT IS ALREADY KNOWN ON THIS TOPIC

⇒ R-115, a HER2-retargeted oncolytic herpes simplex virus expressing IL-12, has shown safety and enhanced efficacy over non-IL-12-expressing variants in immunocompetent mice. However, its activity had been tested in models implanted only with $HER2^+$ cells, not reflective of HER2 heterogeneity in patient tumors.

WHAT THIS STUDY ADDS

⇒ This study shows that R-115 remains effective in a HER2-heterogeneous glioblastoma model, increasing survival and eradicating tumors in a subset of mice. It also proves that the immune system plays a key role, enabling rejection of HER2-negative cells and inducing long-term immune memory.

HOW THIS STUDY MIGHT AFFECT RESEARCH, PRACTICE OR POLICY

⇒ These results support the clinical translation of R-115, suggesting it may benefit patients with tumors partially expressing HER2.

INTRODUCTION

Glioblastoma is the most common and the most aggressive tumor of the central nervous system. Up to 45% of malignant primary brain tumors are glioblastomas[1] and its incidence rate is about 4 cases per 100,000 with an increasing trend.[2 3] The 5-year survival rate of glioblastoma patients is still approximately 5.5% in the USA, with a median overall survival of about 1 year, positively correlated to the extent of surgical resection.[4 5] Standard-of-care treatment for glioblastoma includes maximal safe resection followed by radiotherapy and temozolomide chemotherapy.[6 7] Despite localized radiation enhances survival rates, it also contributes to the transition toward a malignant mesenchymal phenotype of cancer cells by affecting the extracellular matrix.[8] The substantial incurability of glioblastoma arises from its resistance to conventional treatments, largely attributed to its capacity to infiltrate the perivascular space and brain parenchyma. This capability is closely associated with molecular

alterations that result in high intratumor heterogeneity.[9] Largely involved in glioblastoma malignancy is also the tumor microenvironment comprising many cell types including myeloid cells/microglia, blood vessels, astrocytes and extracellular matrix.[10] Glioblastoma is widely acknowledged as an immunosuppressive tumor and there is increasing evidence suggesting that interactions between the tumor microenvironment and tumor cells contribute to immune suppression.[11]

To address these limitations, various approaches are under investigation, focusing on reprogramming the immune system. The goal of immunotherapy is to obtain a proper activation of the immune system without major off-target effects.[10] So far, many immunotherapeutic drugs have been investigated for the treatment of glioblastoma including antibodies targeting specific tumor receptors and antibody targeting immune checkpoint.[11–13] Other promising approaches are based on adoptive cell transfer as well as therapeutic vaccination but they are still facing limitations due to glioblastoma high intratumor heterogeneity.[14–17]

A good alternative to counteract the molecular and pathological characteristics of glioblastoma, circumventing the above-mentioned limitations, is based on oncolytic immunovirotherapy. This approach combines the killing activity of viruses to the stimulation of the immune system as a consequence of their infection and to their ability to carry functional genes, including immune-stimulating factors.[18–21]

Several oncolytic viruses have been tested to treat glioblastoma and some of them have entered clinical trials.[22–26] Of all oncolytic viruses, herpes simplex viruses (HSVs) are among the most investigated and appear to be highly promising. These viruses show many advantages as oncolytic agents, as they can infect both replicating and non-replicating cells, have the potential for the incorporation of a large amount of foreign DNA and any undesired infection or toxicity from the virus replication can be controlled by effective antiviral agents.[27] Additionally, lytic infection by HSV usually kills target cells rapidly and can induce strong immunogenicity that is beneficial when developing vaccine vectors or anticancer agents.[28] A number of oncolytic HSV (oHSV) have been engineered to treat glioblastoma and evaluated in clinical trials showing efficacy and encouraging results.[26 29] Even if most of them are still under evaluation, G47Δ, a third-generation, triple-mutated oncolytic herpes simplex virus type 1 engineered for enhanced tumor selectivity and safety, was recently approved as the first oncolytic viral therapy in Japan for the treatment of brain tumors.[30 31]

The retargeted oHSVs (ReHVs) have been generated in our laboratories to specifically infect only cancer cells expressing selected target molecules. This has been achieved by engineering the coding sequence of the gD protein, through which HSV-1 normally binds its natural receptors, nectin-1 and HVEM. As a result, the ReHV can no longer infect cells via the ubiquitous nectin-1 and HVEM receptors, but is able to enter exclusively into cells expressing the chosen target.[32–35] We recently obtained a proof of concept of the preclinical efficacy of R-115, a ReHV readdressed to HER2 (a member of epidermal growth factor receptor family that is expressed by several tumors including glioblastoma[36]) and armed with murine interleukin-12 (mIL-12).[37] IL-12 is a cytokine capable of strongly stimulating immune cells promoting cytotoxicity and antitumor activity.[38] R-115 was used for the treatment of a glioblastoma murine model where all the tumor cells were engineered to express HER2. Our data showed that R-115 prolonged survival, eradicated about one-fourth of tumors and established an antitumor immune memory.[37] The main strength of R-115 eradication activity was due to its ability to induce an antitumor immune response. In comparison, an almost identical ReHV lacking mIL-12 (R-LM113), when employed in the same context, prolonged survival but failed to eradicate the glioblastoma in any animal.[37 39 40]

Here we analyze the effectiveness of R-115 in a more realistic framework where only a fraction of the tumor cells is targetable by the ReHV, hence validating its efficacy as an agnostic vaccination against glioblastoma potentially useful also against relapses.

MATERIALS AND METHODS

Cell culture

Murine high-grade glioma (mHGG) cells were derived from murine gliomas generated using murine neural progenitor cells transduced with a viral vector expressing PDGF-B and the DsRed reporter gene. The mHGG-HER2 cells were then generated by the transfection of HER2 of mHGG cells.[37 39] When implanted, these cells give rise to tumors that recapitulate the histopathological features of high-grade gliomas, as previously described.[41] Cells were cultured onto plates coated with Matrigel matrix (1:200, BD Bioscience) in Dulbecco Modified Eagle Medium (DMEM)/F12 GlutaMAX™ (Gibco-Life Technologies) added with B27 supplement (Gibco-Life Technologies), recombinant human FGF2 (10 ng/mL, PeproTech), and recombinant human EGF (10 ng/mL, PeproTech).

Splenocytes were obtained by mechanical dissociation in RPMI 1640 GlutaMAX medium (Gibco-Life Technologies), filtered through 40 µm strainer and depleted of erythrocytes using the erythrocyte lysis buffer (NH_4Cl 155 mM, $KHCO_3$ 10 mM, EDTA 0.1 mM).

Syngeneic mouse healthy fibroblasts (referred to as H-Fib) were isolated from adult mice ears. Tissues from BALB/c ears were cut into pieces and treated with collagenase type II (2000U/mL, Worthington Biochemical) in Hanks' Balanced Salt Solution (HBSS, Gibco-Life Technologies) for 25 min at 37°C. After two washes with HBSS, the samples were treated with 0.25% trypsin (Gibco-Life Technologies) for 20 min at 37°C. The cell suspension was filtered through a 40 µm strainer, and the obtained fibroblasts were maintained in DMEM GlutaMAX high glucose (Gibco-Life Technologies) with 10% fetal bovine serum (Gibco-Life Technologies).

Co-cultures were set up in 96-well plates seeded with 2.3×10^5 splenocytes plus 4.5×10^4 mHGG-HER2, 4.5×10^4 mHGG or 5×10^3 mouse fibroblasts when experiments were stopped after 3 days and with 2.3×10^5 splenocytes plus 4.5×10^3 mHGG, 4.5×10^3 mHGG-HER2 or 5×10^3 when experiments were stopped after 7 days. Co-cultures were kept in Matrigel-coated plates (1:200; BD Biosciences) with DMEM/F12 GlutaMAX (Gibco-Life Technologies) added with B27 supplement (Gibco-Life Technologies), recombinant human FGF2 (10 ng/mL, PeproTech), and recombinant human EGF (10 ng/mL, PeproTech).

Animal procedures—murine model of mHGG

The experiments were performed with the BALB/c mouse strain using animals of either sex. Tumors were implanted by injecting a suspension of a total of 2×10^4 mHGG-HER2 or mHGG+mHGG-HER2 (10^4+10^4) cells in adult mice brains using a Hamilton syringe (Bregma coordinates: anterior–posterior, 1.0 mm anterior; lateral, and 2.5 mm below the skull surface). After 8 and/or 21 days post-tumor implantation, mice were randomized and treated intratumorally with 1–3 µL of ReHV preparation, containing 10^6–10^7 PFU of R-115 whose construction and production are described elsewhere.[42] After 120 days post-tumor transplantation, a rechallenge was performed by transplanting a suspension of 2×10^4 mHGG cells into the contralateral hemisphere. Animals were monitored daily and were sacrificed at first signs of suffering or neurological symptoms. Mice which didn't show any symptoms after 120 days post rechallenge received a subcutaneous booster of 5×10^5 mHGG and were sacrificed after 7 days. Control mice of the intracranial and subcutaneous rechallenges were age-matched. Brains collected from sacrificed mice were photographed by a Leica MZ10F fluorescence stereomicroscope. All animals developed tumors and there were no exclusions from the analysis, provided that biological samples were available. To minimize potential confounders, cage positions were varied to avoid location-related bias, and the same operators were consistently involved across the different experimental sessions of the same study.

Immunostaining and flow cytometry

For histological analyses, brains were fixed with 4% paraformaldehyde (Sigma-Aldrich) then cryoprotected in 20% sucrose (Sigma-Aldrich), embedded in O.C.T. (Bio-Optica), and sectioned with a Leica CM3050 S cryostat. The detection of HER2 in brain sections was performed using Herceptin (20 mg/mL, 1:2000, Genentech-Roche) followed by goat anti-human Alexa Fluor 647 (1:1000, A21445, Invitrogen). Immune markers were detected with anti-mouse CD4 (1:100, 550280, BD Pharmigen), APC anti-mouse F4/80 (1:20, 123115, BioLegend), Brilliant Violet 421 anti-mouse/human CD11b (1:100, 101251, BioLegend) and MHC Class II (I-A/I-E) (M5/114.15.2) (1:100, 14-5321-82, eBioscience) followed by secondary staining with Alexa Fluor 488-conjugated AffiniPure Goat Anti-Rat IgG (H+L) (1:400, 112-545-167, Jackson Immunoresearch Laboratories). Nuclei were stained with Hoechst (1 µg/mL, 33342, Sigma-Aldrich). Stained slides were photographed by confocal microscope (Nikon Ti2 LSCM).

To detect specific antibodies against tumor cells produced following immunostimulation by R-115, blood samples were collected from sacrificed mice in 10 mM EDTA, centrifuged, and the resulting supernatant plasma samples were collected and frozen. For the immune-cytofluorimetric staining, 10 µL of plasma were diluted in saline solution and incubated with target cells followed by a secondary staining with a panel of IgGs: Brilliant Violet 421 anti-mouse IgG1 (1:500, 406615, Biolegend), APC/Fire 750 anti-mouse IgG2a (1:500, 407123, Biolegend), APC anti-mouse IgG2b (1:500, 406711, Biolegend) and Alexa Fluor 488 anti-mouse IgG3 (1:500, A21151, Invitrogen).

To analyze cell proliferation, freshly collected splenocytes were stained with 5(6)-carboxyfluorescein diacetate succinimidyl ester (CFDA-SE, Invitrogen). Cells were then harvested 7 days post co-culture and stained with APC-conjugated anti-mouse CD45 antibody (1:800, 559864, BD Biosciences) to evaluate the total proliferating splenocytes or with PE anti-mouse CD45 Antibody (1:5000, 103105, Biolegend), APC anti-mouse CD8a Antibody (1:500, 100711, Biolegend), APC anti-mouse CD19 Antibody (1:1000, 115511, Biolegend), or rat Anti-Mouse CD4 (1:800, 550280, BD Pharmingen) to evaluate splenocytes subpopulations. The binding of the primary anti-mouse CD4 antibody was revealed with a secondary antibody anti-rat CF 660R (1:400, 20390, Biotium).

The normalized amount of proliferating cells (CFDA-SE negative) was obtained with the ratio between the percentage of proliferating splenocytes co-cultured with tumor cells and the percentage of proliferating splenocytes co-cultured with syngeneic mouse fibroblasts (H-Fib).

To analyze splenocytes subpopulation and immune modulation, freshly collected splenocytes were stained with APC anti-mouse F4/80 (1:400, 123115, Biolegend), APC anti-mouse NKp46 (1:400, 137607, Biolegend), APC anti-mouse CD8a (1:500, 100711, Biolegend), APC anti-mouse CD19 (1:1000, 115511, Biolegend), Alexa Fluor 488 anti-mouse CD4, (RM4-5) (1:800, 100532, Biolegend), PE anti-human/mouse Granzyme B (1:100, 372208, BioLegend) and PE anti-mouse Arginase 1 (1:400, 12-3697-82, Invitrogen).

For the detection of MHC-I expression, cells were harvested after 3 days of co-culture and stained with APC-conjugated anti-mouse CD45 antibody (1:800, 559864, BD Biosciences) and with anti-mouse MHC-I (1:100, 14-5999-81, Invitrogen). Binding of the primary antibody was revealed with secondary antibody Alexa Fluor 488-conjugated AffiniPure Goat Anti-Mouse IgG (1:400, 115-545-166, Jackson Immunoresearch Laboratories).

To detect splenocytes-induced tumor cell death, cells were stained 7 days post co-culture with APC-conjugated

anti-mouse CD45 antibody (1:100, 559864, BD Biosciences). After the staining, NIH/3T3 cells (DsRed-negative/CD45-negative) were added as internal normalizer. The percentage of DsRed-positive/CD45-negative (mHGG-HER2 or mHGG) tumor cells over the percentage of DsRed-negative/CD45-negative (NIH/3T3) was considered. Secondarily, the obtained percentage was normalized to the one obtained when tumor cells were cultured alone.

FlowJo software V.10.8 was used for flow cytometry data analyses.

ELISA

Splenocytes were co-cultured for 7 days with mHGG, mHGG-HER2 or H-Fib. Supernatants were then centrifuged, collected and frozen. Mouse Granzyme B Uncoated ELISA Kit (88-8022, Invitrogen), Mouse TNF-α ELISA Flex (3511-1H, Mabtech) and Mouse IFN-γ ELISA Flex (3321-1H, Mabtech) were used in accordance with manufacturer instructions. Adsorbances were read with a BioTek plate reader (EL808 microplate reader, BioTek). Sample concentrations were estimated based on a standard curve, corrected from background and calculated with a local polynomial regression in R (Locally Estimated Scatterplot Smooting).

ELISpot

ELISpot assays were performed using the Mouse IFN-γ ELISpotPLUS kit (3321-4APT-2, Mabtech) in accordance with manufacturer instructions. A 96-well plate was coated with a mouse monoclonal antibody against IFN-γ and 2×10^5 freshly collected splenocytes were seeded. After 48 hours, splenocytes were removed and spots were revealed by Elispot reader (Automated Elisa-Spot Assay Video Analysis Systems). Positive responses were considered those whose intensity distributions were >10 spots. The mean number of spots was calculated, corrected from background, and normalized on the medium spot intensity of scNAIVE mice.

Luciferase assay

Murine HGG cells were transduced to express the firefly luciferase and puromycin resistance and were then selected using puromycin 1 mg/L to obtain an engineered mHGG line stably expressing luciferase (mHGG-LUC). For this assay, 1.15×10^6 splenocytes were co-cultured with 2.3×10^5 mHGG-LUC for 7 days then cells were harvested, washed twice with Phosphate Buffer Saline (Gibco-Life Technologies) and lysed (E195A, Promega). Lysates were then incubated with luciferin (E151A, Promega) at a 1:4 ratio. The amount of light emitted was measured with a luminometer (GloMax 20/20, Promega) and represented as Relative Luminescence Units (RLU). Values from co-cultured lysates were normalized on those obtained with lysates derived from mHGG-LUC cells cultured alone.

Statistical analysis

Sample sizes for each experiment are indicated in the results section. Survival analyses were performed with the Log-Rank (Mantel-Cox) test. Statistical analyses were performed with a two-sided t-test when between two conditions or one-way analysis of variance followed by Tukey's multiple comparison test when between more conditions.

Principal component analysis (PCA) was performed on different sets of observations using the prcomp function of stats R package. For each subset of observations, samples retaining 4% or more missing values were discarded, and the remaining data were scaled and centered using z-score normalization. The remaining missing values were imputed using the median by the naniar R package.[43]

Statistical significance is represented as follows: ****p<0.0001, ***p<0.001, **p<0.01, *p<0.05.

All data were analyzed with GraphPad Prism V.10.1.0 and R V.4.1.2.

RESULTS

Multiple administrations of R-115 do not significantly change its efficacy

Our previous results demonstrated that administering R-115 21 days (late treatment) after orthotopic transplantation of mHGG cells expressing HER2 (mHGG-HER2) extended the survival of treated mice and eliminated the tumor in approximately one quarter of them.[37] Here, we assessed if R-115 efficacy might be affected by modifications in the timing and doses. For this investigation, we tested two additional R-115 administration paradigms: single treatment at 8 days (early treatment) and double treatment at 8 and 21 days (early+late treatment) post-tumor transplantation (figure 1A). BALB/c mice were orthotopically transplanted with 2×10^4 mHGG-HER2 cells and then treated with R-115 according to the schedules. As shown in figure 1B, median overall survival time of both R-115-treated arms (early treatment=46.5 days; early+late treatment=70 days) was increased respectively by 1.4 and 2.1 times in comparisons to the control group (CTR vs early treatment: log-rank (Mantel-Cox) test p<0.0001, CTR versus early+late treatment: log-rank (Mantel-Cox) test p<0.0001). On the other hand, the analyses showed that the difference between the three treatments (early, early+late and late) is not significant (at least for HR>0.35, with a power of 80%).

R-115 exerts a similar protection against HER2-homogeneous and HER2-heterogeneous glioblastomas

A major concern in envisaging a translation of oHSVs, including ReHVs treatment to patients is the intrinsic heterogeneity of the glioblastoma masses. All the above-mentioned results were obtained by treating tumors composed homogeneously of cells expressing HER2. However, glioblastomas are not expected to be composed of cells that uniformly express any specific marker molecule. To address this point, we examined the performance of our treatment on a mixed population of cells, some of which express HER2 and others do not, with the aim of mimicking the heterogeneity of HER2 expression observed in patients. We therefore orthotopically transplanted

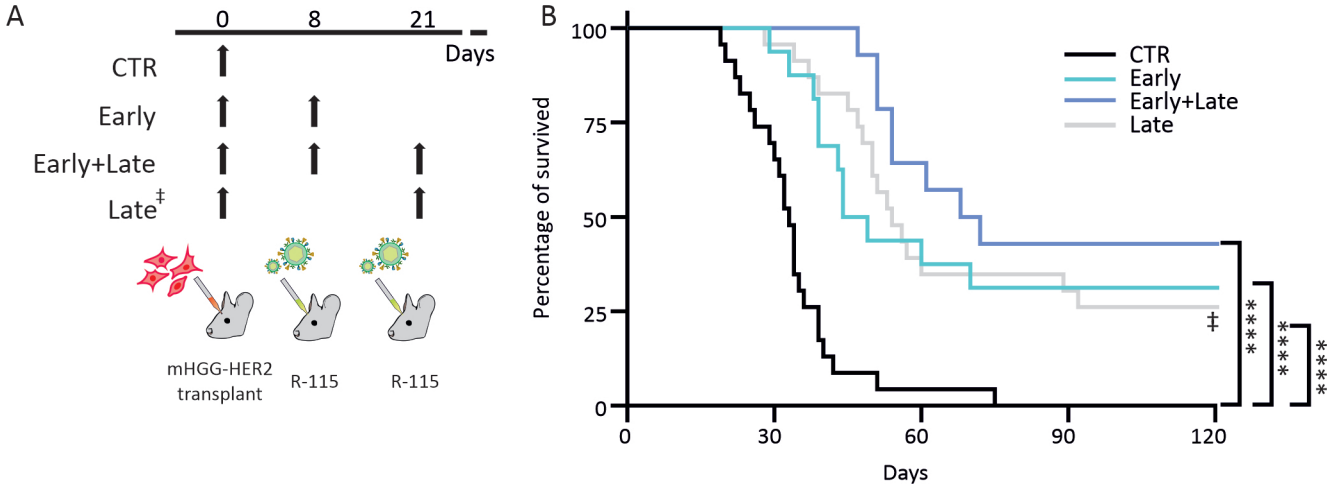

Figure 1 Effect of different administration schedules of R-115 on mHGG-HER2-bearing mice. (A) A cartoon displaying the experimental design of the ReHV treatments on mice transplanted with mHGG-HER2. (B) Kaplan-Meier survival curves derived from the experiments shown in (A). Mice were treated with R-115 according to two alternative administration schedules: 8 days (sky blue line, n=16) or 8 and 21 days (dark sky-blue line, n=14) post-tumor inoculation (corresponding to 0 days). The gray line labeled with ‡ represents data from Alessandrini *et al*,[37] where mice were treated 21 days post-transplantation for a direct comparison. The control arm is shown as a black line (n=23). Kaplan-Meier curves were analyzed by log-rank (Mantel-Cox) test ****p<0.0001. mHGG, Murine high-grade glioma; ReHV, retargeted oncolytic herpes simplex virus.

BALB/c mice with 10^4 mHGG plus 10^4 mHGG-HER2 cells (hereinafter referred to as mHGG-MIX) and treated them with the same R-115 schedules tested on homogeneous mHGG-HER2. Remarkably, the results closely resembled those achieved when treating fully targetable mHGG-HER2 bearing mice. The overall survival of the mHGG-MIX treated mice was increased compared with controls (from 39 to 75 days, log-rank (Mantel-Cox) test p<0.0001) and 12 animals (30%) were still alive 120 days after tumor transplant. These data show that R-115 efficacy on mHGG-MIX bearing mice was at least as good as on the mHGG-HER2 (figure 2A) and, once again, modifying the treatment schedule did not affect the outcome, not even when treating with R-LM113 not expressing IL-12 (online supplemental figure 1). The similar therapeutic efficacy observed in mixed and homogeneous $HER2^+$ tumors is consistent with the similar presence of immune cell infiltrates within the HER2-positive and HER2-negative regions of mHGG-MIX tumors (online supplemental figure 2), indicating that immune cells are equally recruited throughout the tumor independently of HER2 expression.

The eradication of an otherwise invariably lethal glioma achieved with R-115 treatment was noteworthy, yet it involved only a fraction of the treated animals. We thus explored whether the partial response to the R-115 treatment in some animals could be due to the loss of the target marker (HER2) following the treatment, so that the tumor can no longer be infected with the appropriate ReHV, thereby rendering the tumor not infectable by the virus. We therefore assessed the expression of HER2 in mice brains. Tumor masses in both R-115 treated (n=15) and control mice (n=6), regardless of whether they were transplanted with HER2-homogeneous or HER2-heterogeneous cell populations, retained a substantial fraction of HER2-positive cells, as determined by immunostaining (figure 2C). These findings suggest that, on the one hand, the partial efficacy of R-115 cannot be attributed to HER2 expression, and, on the other hand, the tumor masses remained potentially subject to R-115 targeting.

R-115 treatment induces a potent immune memory against mHGGs

The advantage of R-115 over the former not armed versions of ReHV R-LM113[37] lies in its capacity to induce mIL-12 expression within infected tumor cells, thus stimulating an immune response. This feature can potentially contribute to establishing an immune memory against tumor neoantigens. To evaluate the development of such an immune memory, we conducted a rechallenge experiment where 2×10^4 mHGG cells (not expressing the HER2 transgene) were intracranially transplanted into the contralateral hemisphere of a subset of mice that had survived more than 120 days from the initial tumor transplant (n=8). A group of age-matched mice was transplanted with the same cells as control (n=8). All mice of the control group died within 51 days while four out of eight previously treated animals were still alive after 120 days (figure 2B). Among the other 4, one died at day 56 post-rechallenge without exhibiting tumor masses, and its death was attributed to causes not correlated to the tumor. The brains of R-115-treated mice cured from both primary and secondary transplants, herein referred to as long survivors (LS_R-115), were examined for the expression of the DsRed reporter gene associated with the tumor cells. figure 2D,E shows that the signal of the DsRed reporter gene was undetectable in cured mice, indicating that R-115 not only induced the eradication

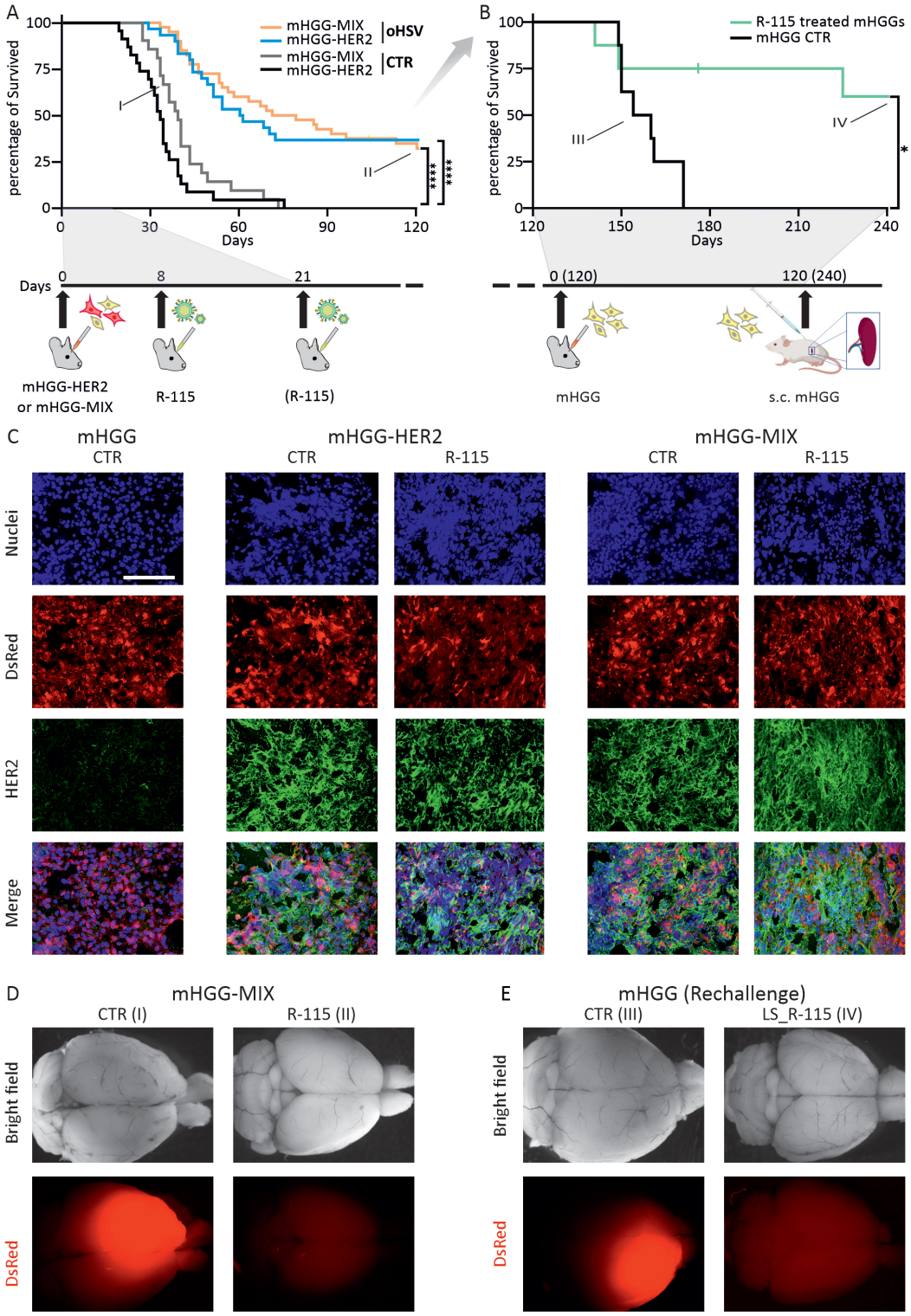

Figure 2 Effects of R-115 on heterogeneous glioblastomas. (A) Kaplan-Meier survival curves of mHGG-transplanted mice: mHGG-HER2 untreated (black line, n=23) and treated with R-115 (blue line, n=30) or mHGG-MIX untreated (gray line, n=21) or treated with R-115 (orange line, n=40). (B) Kaplan-Meier survival curve of mice rechallenged with an injection of mHGG, 120 days after the first tumor transplant (green line, n=8). Aged-matched control animals transplanted with mHGG are shown as a black line (n=8). Kaplan-Meier curves were analyzed by log-rank (Mantel-Cox) test. (C) Representative immunostaining of brains from mice bearing mHGG, mHGG-HER2 or mHGG-MIX, treated as specified. Nuclei are shown in blue, DsRed tumor-cell reporter is shown in red and HER2 immunoreactivity is shown in green. Scale bar=100 µm. (D) Representative dorsal images of brains from mice of the mHGG-MIX control arm (I) or R-115 treated arm (II) and (E) images of brains from mice of the mHGG rechallenge control arm (III) or R-115 treated and rechallenged arm (IV). These mice correspond to the events labeled as I, II, III and IV in Kaplan-Meier curves in (A, B). In all micrographs, the red channel shows the DsRed fluorescent reporter expressed by the tumor cells. *p<0.05, ****p<0.0001. mHGG, Murine high-grade glioma.

of the initially transplanted tumor but also promoted the rejection of a second tumor transplant.

Long-term effects of R-115 on the immune system

To analyze the reactivity of the immune system of long survivors against tumor cells, we boosted them with a subcutaneous injection of 5×10^5 mHGG cells. In parallel, as a control, age-matched naive mice received the same subcutaneous injection (scNAIVE, n=6). The basal reactivity of age-matched naive mice was also tested (NAIVE, n=4; see online supplemental figures).

After 7 days from subcutaneous injection, we sacrificed all the mice and collected their splenocytes, plasmas, and brains. The same samples were collected from mice treated with ReHVs that died because of the tumor (hereinafter named as "not-long survivors treated with R-115"; NLS_R-115) and control mice (ie, mice intracranially injected with the tumor cells that did not receive the treatment, CTR) when they developed neurological symptoms (figure 3B).

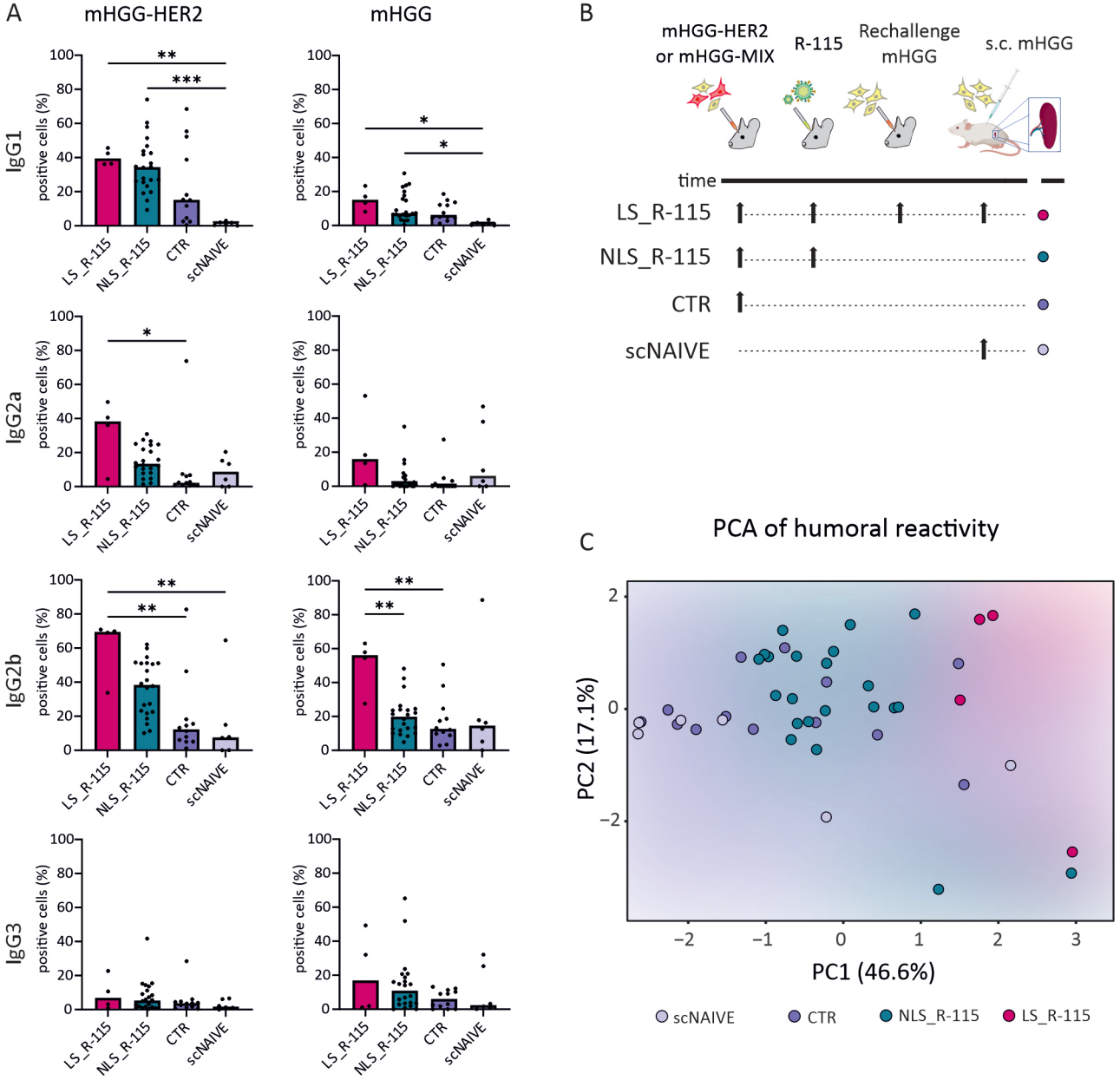

Figure 3 Humoral reactivity against mHGG-HER2 and mHGG tumor cells. (A) Reactivity of IgG1, IgG2a, IgG2b, and IgG3 against mHGG-HER2 or mHGG. LS_R-115 n=4, NLS_R-115 n=22, CTR n=12, scNAIVE n=6. Data are represented as a scatter plot with bars (median) and analyzed with one-way ANOVA followed by Tukey's multiple comparison test. *p<0.05, **p<0.01, ***p<0.001. (B) Scheme of tumor transplant, ReHV treatment, orthotopical rechallenge, and subcutaneous booster according to each analyzed group. (C) PCA of all the data about humoral reactivity in all analyzed groups. ANOVA, analysis of variance; mHGG, Murine high-grade glioma; NLS_R-115, not-long survivors treated with R-115; PCA, principal component analysis; ReHV, retargeted oncolytic herpes simplex virus.

To characterize the immune elements involved in the immune response and memory, we examined both the humoral and the cytotoxic component.

The humoral response following R-115 treatment was assessed by evaluating the production of antibodies reacting against tumor cells. Plasma obtained from mice at the time of sacrifice was incubated with mHGG-HER2, mHGG, or syngeneic healthy fibroblast (hereinafter referred to as H-Fib) and the binding of specific IgG1, IgG2a, IgG2b, and IgG3 to these cells was examined (figure 3A and online supplemental figure 3). The results indicated a general increasing trend in tumor-specific antibody production in the R-115 treatment groups (NLS_R-115 and LS_R-115) vs the control groups (CTR and scNAIVE and NAIVE). IgG1, IgG2a, and IgG2b showed the highest differences between groups; however, when plasmas were tested on mHGG cells, they showed a general decreased reactivity. Nevertheless, IgG2b still exhibited good specific reactivity against tumor cells, although they also displayed, to a lesser extent, increased nonspecific reactivity when tested against H-Fib (online supplemental figure 3A). Despite a general partial response, a PCA including all the data about humoral reactivity showed that the differences between groups are not very pronounced, suggesting that the humoral component is unlikely to be the main driver of the anticancer activity exerted by R-115 (figure 3C).

We then evaluated if the immune response was associated with an increased proliferation of immune cells by staining freshly collected splenocytes with CFDA-SE and then co-culturing them with mHGG-HER2, mHGG, or H-Fib. After 7 days of co-culture, cells were stained with CD45 and the amount of proliferating CD45-positive cells was evaluated (figure 4A). Despite at the time of sacrifice, there was no difference in the amount of splenocyte populations between tested groups (online supplemental figure 4), splenocytes derived from LS_R-115 mice showed an increased proliferation in comparison to that of CTR and scNAIVE mice. To characterize respectively the proliferation of T helper-, T cytotoxic-, and B-lymphocytes, co-cultured splenocytes isolated from LS_R-115 and scNAIVE mice were also stained for CD4, CD8, or CD19. The three lymphocyte subpopulations originating from long survivors exhibited higher levels of proliferation compared with those derived from scNAIVE (figure 4C and online supplemental figure 5), while there is no difference between scNAIVE and NAIVE except for CD4 co-cultured with mHGG-HER2 (online supplemental figure 6A). The increase in proliferation was observed indistinctly whether the lymphocytes were co-cultured with either mHGG-HER2 cells or mHGG cells.

We then evaluated possible mediators involved in the immune response elicited by R-115. First, we assayed the release of IFN-γ by freshly collected splenocytes from LS_R-115, scNAIVE, and NAIVE experimental groups. These analyses showed that splenocytes from LS_R-115 mice released a higher amount of IFN-γ compared with those from control groups, underlining their prompt responsiveness to the subcutaneous injection (online supplemental figure 6C).

To assess whether the activity of splenocytes was specific for glioblastoma cells, we quantified the levels of Granzyme B, TNF-α, and IFN-γ in the conditioned medium of splenocytes derived from the different experimental mouse groups co-cultured with mHGG-HER2, mHGG, and H-Fib. As depicted in figure 4D, a modest or nearly absent release of immune mediators was exhibited by splenocytes from all tested groups but those derived from LS_R-115 co-cultured with mHGG-HER2 or mHGG. There was almost no release of Granzyme B, TNF-α, and IFN-γ by NAIVE mice when co-cultured with tumor cells, and low levels, similar to those exhibited by splenocytes from control groups, were released by LS_R-115 when co-cultured with H-Fib (online supplemental figure 6B). Consistently, the increased release of Granzyme B correlated with the higher intracellular levels of Granzyme B detected at the time of sacrifice within both $CD8^+$ T cells and NK cells derived from long-surviving mice (online supplemental figure 4).

Immune-mediated effects on tumor cells

Having characterized the effects induced by R-115 treatment on immune cells, we then tested if these changes led to the reversion of the immune-evasive phenotype of glioblastoma and the actual killing activity of tumor cells. Glioblastoma cells are often characterized by a diminished expression of MHC-I, a condition that is well portrayed by our model where both mHGG-HER2 and mHGG cells exhibit significantly low levels of MHC-I (online supplemental figure 7B). To explore whether splenocytes could reinstate MHC-I on tumor cells, we examined its expression in tumor cells after 3 days of co-culture. The analysis revealed the reestablishment of MHC-I on both mHGG-HER2 and mHGG cells when co-cultured with LS_R-115 splenocytes and, to a lesser extent, with NLS_R-115; in contrast, the co-culture with splenocytes from CTR, scNAIVE, or NAIVE mice had minimal or no impact (see figure 5A,B, online supplemental figure 7A). To assess the cytotoxicity of splenocytes, we leveraged the DsRed reporter gene expressed by tumor cells and determined the fraction of DsRed-positive cells left after 7 days of co-culture. As shown in figure 5C,D and online supplemental figure 7C), tumor cells reduction mirrored the MHC-I expression, resulting in a significant decrease of tumor cells co-cultured with splenocytes from LS_R–115 and, to a lesser extent, with NLS_R-115. The specific recognition of new antigens, other than HER2, and the subsequent killing mediated by splenocytes were further investigated in mHGG cells. These cells were engineered to induce the expression of the luciferase reporter gene (mHGG-LUC), and the luciferase activity was used to quantify their amount in the co-cultures. This experiment confirmed that glioblastoma cells sharply diminished when co-cultured with splenocytes from LS_R-115 (see online supplemental figure 7D).

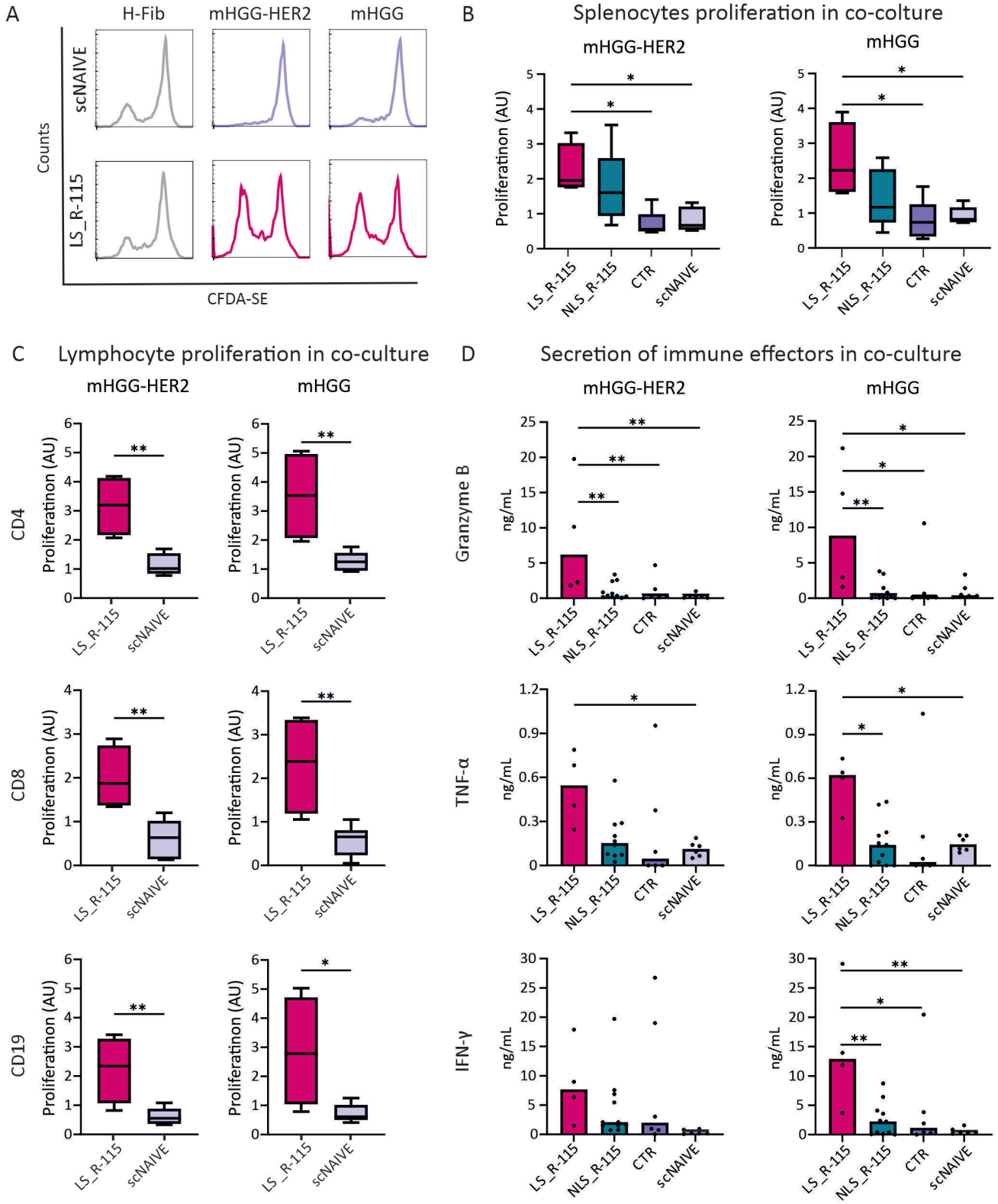

Figure 4 R-115 effects on the immune components. (A) Representative flow cytometry histograms of CFDA-SE proliferating splenocytes derived from LS_R-115 and scNAIVE co-cultured with mHGG-HER2, mHGG or control (H-Fib). (B) Box plot of proliferating splenocytes co-cultured with mHGG-HER2 or mHGG tumor cells. LS_R-115 n=4, NLS_R-115 n=15, CTR n=5, scNAIVE n=6. (C) Box plot of proliferating CD4, CD8 and CD19 lymphocytes co-cultured with mHGG-HER2 or mHGG tumor cells. LS_R-115 n=4, scNAIVE n=6. (D) Scatter plot with bars (median) of Granzyme B, TNF-α, and IFN-γ released by splenocytes co-cultured with mHGG-HER2 or mHGG. LS_R-115 n=4, NLS_R-115 n≥10, CTR n=6, scNAIVE n=6. Data are analyzed with one-way ANOVA followed by Tukey's multiple comparison test or with two-sided t-test. *p<0.05, **p<0.01. ANOVA, analysis of variance; mHGG, Murine high-grade glioma; NLS_R-115, not-long survivors treated with R-115; ReHV, retargeted oncolytic herpes simplex virus.

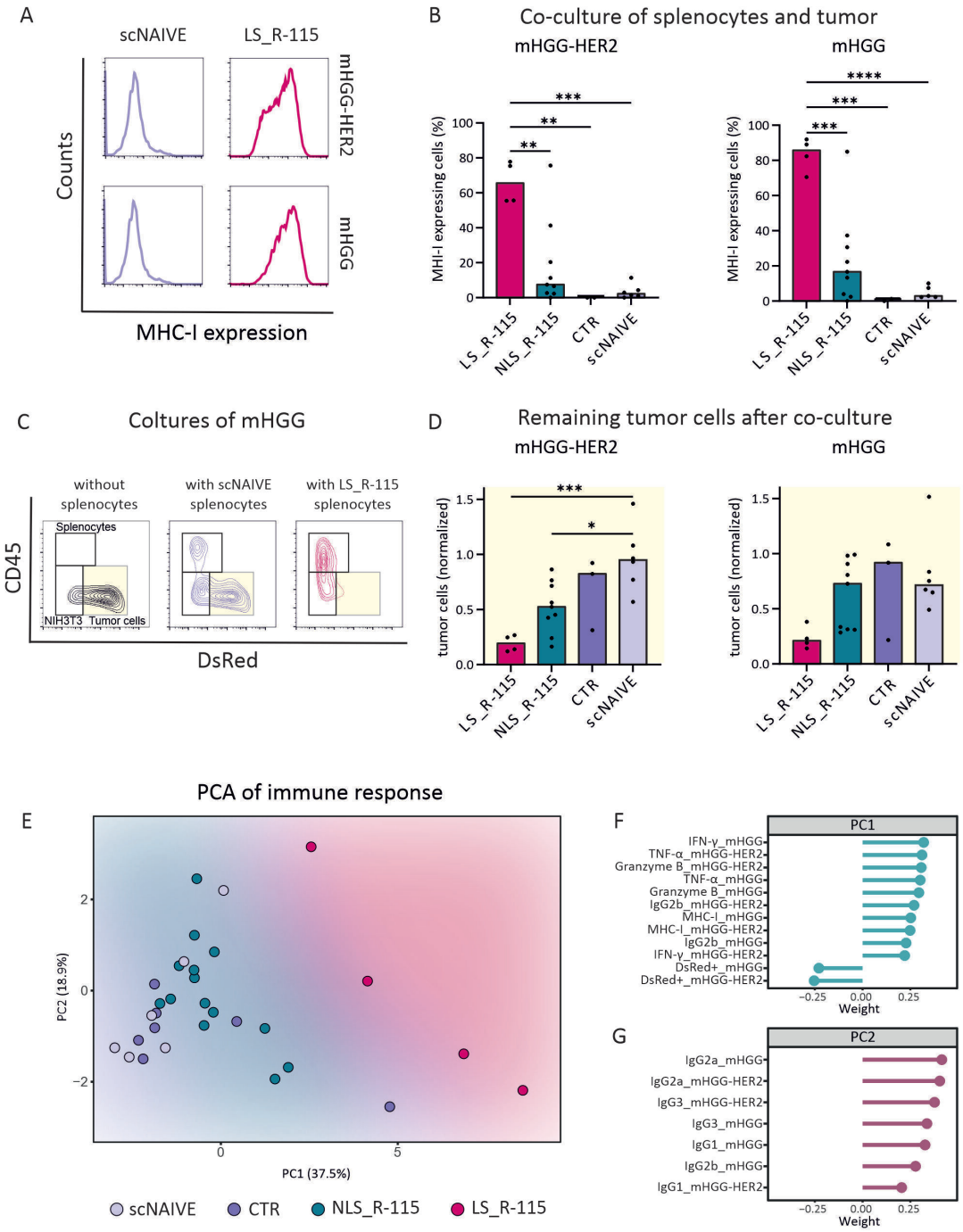

Figure 5 Immune response impact on tumor cells and comprehensive ReHV-mediated response. (A) Representative flow cytometry histograms of MHC-I expression on mHGG-HER2 or mHGG co-cultured with splenocytes derived from scNAIVE or LS_R-115. (B) Scatter plot with bars (median) showing the percentage of co-cultured mHGG-HER2 or mHGG MHC-I expressing cells. LS_R-115 n=4, NLS_R-115 n=9, CTR n≥2, scNAIVE n≥5. (C) Schematic representation of the strategy used to analyze the decrease of glioma cells when co-cultured with splenocytes from the specified sources. The analysis relied on measuring the ratio between the number of glioma cells and the number of NIH/3T3 cells added at a standardized amount as internal normalizer. DsRed intensity was used to identify glioma cells (mHGG or mHGG-HER2), CD45 intensity was used to discriminate splenocytes from NIH/3T3 cells and tumor cells. (D) Scatter plot with bars (median) showing mHGG-HER2 or mHGG tumor cells left after co-culture with splenocytes. Values are reported as normalized to parallel cultures of tumor cells without splenocytes. LS_R-115 n=4, NLS_R-115 n=9, CTR n=3, scNAIVE n=6. (E) Principal Component Analysis showing all the analyzed antitumoral features (specific IgG, splenocytes proliferation, immune mediators release, MHC-I expression by tumor cells and tumor DsRed-positive cells left). LS_R-115 n=4, NLS_R-115 n=14, CTR n=7, scNAIVE n=6. (F, G) Highlight the most relevant features constituting the PC1 and PC2, respectively, of the PCA shown in (E). Data in (B, D) were analyzed with one-way ANOVA followed by Tukey's multiple comparison test. *p<0.05, **p<0.01, ***p<0.001, ****p<0.0001 . ANOVA, analysis of variance; mHGG, Murine high-grade glioma; NLS_R-115, not-long survivors treated with R-115; PCA, principal component analysis; ReHV, retargeted oncolytic herpes simplex virus.

Finally, we summarized all observations obtained from our assays using PCA to assess how the observed immune responses could distinguish the different experimental groups. As shown in figure 5E and online supplemental figure 7E, samples segregate in a group-dependent manner. At one extreme of the PC1/PC2 graph, predominantly control samples (scNAIVE, NAIVE, and CTR) are observed, while an intermediate region shows a predominance of NLS_R-115 samples. All LS_R-115 samples were located at the opposite extreme. This pattern of segregation suggests that the treatments significantly influence immune responses, indicating a gradation in the impact from control to NLS_R-115 and peaking with LS_R-115. These findings imply that the mechanisms distinguishing NLS_R-115 from control samples are amplified in LS_R–115 samples.

DISCUSSION

We previously demonstrated the efficacy of R-115 virus for the treatment of immunocompetent mice inoculated with syngeneic high-grade glioma cells expressing HER2.[37] The employed virus is an oncolytic HSV retargeted to HER2 and armed with murine IL-12. The aim of the current work was to assess the efficacy of the treatment in a more complex system where only a fraction of cells expressed the targetable receptor. Such a system, based on immunocompetent mice transplanted with high-grade gliomas resembling the immune-pathological features of human tumors, mirrors human glioblastomas that display a high intra-tumor heterogeneity with cells expressing different markers at different levels.

Here we demonstrated that the treatment with R-115 is remarkably effective even in a model where only half of the cells can be directly infected and killed by the ReHV, mHGG-MIX (mHGG-HER2+mHGG). Actually, the performance of R-115 on homogeneously HER2-expressing cells was virtually indistinguishable from that on mHGG-MIX, both in terms of survival and percentage of fully rescued mice. Specifically, the median overall survival of ReHV-treated mice previously injected with mHGG-MIX was almost doubled compared with untreated mice, and the percentage of cured mice was still about one fourth, suggesting promising potential for R-115 as a therapeutic agent. Also, the proposed treatment showed strong stability when doses and timing are modulated.

Our results indicate that R-115 immunovirotherapy allowed us to establish a solid immune memory that prevented the growth of the majority of secondary transplanted tumors. These results are further sustained by our previous findings in other murine models which demonstrated, using R-115 or other ReHSV, that oncolytic immunotherapy can vaccinate against tumor antigens not targetable by the virus.[33–35]

We also characterized the specific immune reaction developed against tumor cells expressing or not expressing the target of the virus, HER2. Altogether, our findings demonstrate that the immune component of R-115-treated mice, which survived both the first and the subsequent second tumor transplant (Long Survivors), was strongly reactive against tumor cells. The characterization of the humoral response showed a high secretion of specific antibodies. We found that the most abundant IgGs highlighting the differences between treated and untreated mice are IgG2b that, together with IgG2a, have been previously reported as the most pro-inflammatory IgGs in the mouse.[44]

The cellular components of the immune system showed a predominant role in the antitumor reaction and immunity. In fact, following co-culture, splenocytes from LS_R–115 and, to a lesser extent, NLS_R-115 treated and not rescued mice exhibited an increased proliferation of $CD4^+$ and $CD8^+$ lymphocytes T and B lymphocytes.

The antitumor activity of splenocytes from Long Survivors was quite evident when we analyzed supernatants derived from their co-culture with tumor cells where we detected an increased amount of various antitumoral immune mediators. In particular, we identified increased release of Granzyme B, which is the most powerful pro-apoptotic granzyme that mediates the killing of target cells when released by cytotoxic lymphocytes inducing an effective death.[45] Supernatant from LS_R-115 also displayed an increased amount of TNF-α, another pleiotropic cytokine which mediates tumor vasculature destruction, induces inflammation-mediated necrosis of tumor cells, is an important mediator of T- and NK-mediated killing of tumor cells, and promotes switching of Tumor Associated Macrophages to an antitumor M1 phenotype.[46 47] We also detected an increased release of IFN-γ, a deeply investigated pleiotropic cytokine known for its antitumor effects[48 49] whose release and activity can be further enhanced by both the HSV infection and IL-12.[25] Despite the role of IFN-γ in cancer still being debated,[49] our results sustain its antitumor activity. All these released cytokines, including ReHV-driven mIL-12, mediate a strong antitumor effect, making their potent inflammatory response fundamental to reawaken the antitumor activity of glioblastoma microenvironment.

The extended multifaceted immune machinery showed that the release of antitumor immune mediators also promoted the restoration of MHC-I on immune-evasive tumor cells, finally mediating their killing.

Remarkably, our separate characterization of the antitumor response activated against both mHGG-HER2 and mHGG tumor cells demonstrated that the therapeutic effects promoted by R-115 include a strong response against neo-antigens capable of preventing the growth also of HER2-negative tumor cells.

Altogether, these results highlight that the role of R-115 for the treatment of glioblastoma is not only the direct targeting of HER2-expressing cells but also the induction of a comprehensive immune response capable of reverting a cold tumor like glioblastoma into a hot one.

Oncolytic virotherapy has already shown clinical efficacy in the treatment of tumors like cutaneous

melanoma, where T-VEC has been employed so far in thousands of patients showing the safety and efficacy of in situ vaccination elicited by oncolytic viruses.[50] Many oncolytic viruses are currently under investigation and have reached clinical trials, but in accordance with the engineered virus employed, there are still limits, often associated with viral spread or limited efficacy. Our preclinical results obtained in an immunocompetent murine model resembling human glioblastoma demonstrate how R-115, remodeled for the expression of human IL-12, is worth being investigated as potential new therapy for the treatment of glioblastoma.

Correction notice This article has been corrected since it was first published online. The email address for the corresponding author Francesca Piaggio has been updated.

Contributors Conceptualization: FP and PM. Data curation: FP, CR, DC, and PM. Methodology: FP, IA, and PM. Investigation: FP, CR, FA, DM, DC, IA, AV, TG, GC-F, and PM. Visualization: FP, DC, and PM. Funding acquisition: FP and PM. Project administration: FP and PM. Writing–original draft: FP, CR, and PM. Guarantor: FP. Artificial intelligence (AI) tools were used to refine the manuscript language and ensure grammatical accuracy in English.

Funding This study was funded by Associazione Italiana per la Ricerca sul Cancro (27852), Progetti di Rilevante Interesse Nazionale 2022 (20224NCSN5), Progetti di Rilevante Interesse Nazionale 2020 (20205TF444), #NEXTGENERATIONEU (NGEU) and funded by the Ministry of University and Research (MUR), National Recovery and Resilience Plan (NRRP), project MNESYS PE0000006 (1553 11.10.2022) and Ministero della Salute (GR-2021-12373325).

Competing interests GC-F is the main inventor in the retargeted HSV technology owned by Università di Bologna and a minor shareholder in Nouscom. All the other authors have no competing interests.

Patient consent for publication Not applicable.

Ethics approval All animal procedures were approved by the internal committee for protection of animals used for scientific purposes (OPBA) of IRCCS Ospedale Policlinico San Martino and by the Italian Ministry of Health according to the Italian law D. lgs. 26/2014, authorization approval number 1044/2020-PR.

Provenance and peer review Not commissioned; externally peer reviewed.

Data availability statement Data are available on reasonable request.

ORCID iDs

Francesca Piaggio https://orcid.org/0000-0003-0379-0047
Chiara Riviera https://orcid.org/0009-0004-5518-9610
Francesco Alessandrini https://orcid.org/0000-0002-8450-848X
Daniela Marubbi https://orcid.org/0009-0005-2565-5681
Davide Ceresa https://orcid.org/0000-0002-2833-4024
Irene Appolloni https://orcid.org/0000-0002-0986-2278
Agnese Vincenzi https://orcid.org/0000-0001-9806-9804
Tatiana Gianni https://orcid.org/0000-0003-1946-2064
Gabriella Campadelli-Fiume https://orcid.org/0000-0002-6012-6081
Paolo Malatesta https://orcid.org/0000-0003-3045-3361

REFERENCES

1 McFaline-Figueroa JR, Lee EQ. Brain Tumors. *Am J Med* 2018;131:874–82.
2 Davis FG, Smith TR, Gittleman HR, *et al*. Glioblastoma incidence rate trends in Canada and the United States compared with England, 1995-2015. *Neuro Oncol* 2020;22:301–2.
3 Sinning M, Frelinghuysen M, Gallegos M, *et al*. Outcome of patients with primary glioblastoma in Chile: single centre series. *Ecancermedicalscience* 2021;15:1184.
4 Luo C, Song K, Wu S, *et al*. The prognosis of glioblastoma: a large, multifactorial study. *Br J Neurosurg* 2021;35:555–61.
5 Brown TJ, Brennan MC, Li M, *et al*. Association of the Extent of Resection With Survival in Glioblastoma: A Systematic Review and Meta-analysis. *JAMA Oncol* 2016;2:1460–9.
6 Komori T. The 2021 WHO classification of tumors. *Brain Tumor Pathol* 2022;39:47–50.
7 Stupp R, Mason WP, van den Bent MJ, *et al*. Radiotherapy plus concomitant and adjuvant temozolomide for glioblastoma. *N Engl J Med* 2005;352:987–96.
8 Yoo K-C, Suh Y, An Y, *et al*. Proinvasive extracellular matrix remodeling in tumor microenvironment in response to radiation. *Oncogene* 2018;37:3317–28.
9 Paw I, Carpenter RC, Watabe K, *et al*. Mechanisms regulating glioma invasion. *Cancer Lett* 2015;362:1–7.
10 Jia Z, Ragoonanan D, Mahadeo KM, *et al*. IL12 immune therapy clinical trial review: Novel strategies for avoiding CRS-associated cytokines. *Front Immunol* 2022;13:952231.
11 Chinot OL, Wick W, Mason W, *et al*. Bevacizumab plus Radiotherapy–Temozolomide for Newly Diagnosed Glioblastoma. *N Engl J Med* 2014;370:709–22.
12 Litak J, Mazurek M, Grochowski C, *et al*. PD-L1/PD-1 Axis in Glioblastoma Multiforme. *Int J Mol Sci* 2019;20:5347.
13 Zhang N, Wei L, Ye M, *et al*. Treatment Progress of Immune Checkpoint Blockade Therapy for Glioblastoma. *Front Immunol* 2020;11:592612.
14 Schumacher TN, Schreiber RD. Neoantigens in cancer immunotherapy. *Science* 2015;348:69–74.
15 Elsamadicy AA, Chongsathidkiet P, Desai R, *et al*. Prospect of rindopepimut in the treatment of glioblastoma. *Expert Opin Biol Ther* 2017;17:507–13.
16 Choi BD, Maus MV, June CH, *et al*. Immunotherapy for Glioblastoma: Adoptive T-cell Strategies. *Clin Cancer Res* 2019;25:2042–8.
17 Wen PY, Reardon DA, Armstrong TS, *et al*. A Randomized Double-Blind Placebo-Controlled Phase II Trial of Dendritic Cell Vaccine ICT-107 in Newly Diagnosed Patients with Glioblastoma. *Clin Cancer Res* 2019;25:5799–807.
18 Asija S, Chatterjee A, Goda JS, *et al*. Oncolytic immunovirotherapy for high-grade gliomas: A novel and an evolving therapeutic option. *Front Immunol* 2023;14:1118246.
19 Feola S, Russo S, Ylösmäki E, *et al*. Oncolytic ImmunoViroTherapy: A long history of crosstalk between viruses and immune system for cancer treatment. *Pharmacology & Therapeutics* 2022;236:108103.
20 Chiocca EA, Rabkin SD. Oncolytic viruses and their application to cancer immunotherapy. *Cancer Immunol Res* 2014;2:295–300.
21 Garmaroudi GA, Karimi F, Naeini LG, *et al*. Therapeutic Efficacy of Oncolytic Viruses in Fighting Cancer: Recent Advances and Perspective. *Oxid Med Cell Longev* 2022;2022:3142306.
22 Martikainen M, Essand M. Virus-Based Immunotherapy of Glioblastoma. *Cancers (Basel)* 2019;11:186.
23 Markert JM, Razdan SN, Kuo H-C, *et al*. A Phase 1 Trial of Oncolytic HSV-1, G207, Given in Combination With Radiation for Recurrent GBM Demonstrates Safety and Radiographic Responses. *Mol Ther* 2014;22:1048–55.
24 Harrow S, Papanastassiou V, Harland J, *et al*. HSV1716 injection into the brain adjacent to tumour following surgical resection of high-grade glioma: safety data and long-term survival. *Gene Ther* 2004;11:1648–58.
25 Patel DM, Foreman PM, Nabors LB, *et al*. Design of a Phase I Clinical Trial to Evaluate M032, a Genetically Engineered HSV-1 Expressing IL-12, in Patients with Recurrent/Progressive Glioblastoma Multiforme, Anaplastic Astrocytoma, or Gliosarcoma. *Hum Gene Ther Clin Dev* 2016;27:69–78.
26 Ling AL, Solomon IH, Landivar AM, *et al*. Clinical trial links oncolytic immunoactivation to survival in glioblastoma. *Nature New Biol* 2023;623:157–66.
27 Robilotti E, Zeitouni NC, Orloff M. Biosafety and biohazard considerations of HSV-1-based oncolytic viral immunotherapy. *Front Mol Biosci* 2023;10:1178382.
28 Jahan N, Ghouse SM, Martuza RL, *et al*. In Situ Cancer Vaccination and Immunovirotherapy Using Oncolytic HSV. *Viruses* 2021;13:1740.

29 Koch MS, Lawler SE, Chiocca EA. HSV-1 Oncolytic Viruses from Bench to Bedside: An Overview of Current Clinical Trials. *Cancers (Basel)* 2020;12:3514.
30 Todo T, Ino Y, Ohtsu H, *et al*. A phase I/II study of triple-mutated oncolytic herpes virus G47Δ in patients with progressive glioblastoma. *Nat Commun* 2022;13:4119.
31 Todo T, Ito H, Ino Y, *et al*. Intratumoral oncolytic herpes virus G47Δ for residual or recurrent glioblastoma: a phase 2 trial. *Nat Med* 2022;28:1630–9.
32 Vannini A, Parenti F, Barboni C, *et al*. Efficacy of Systemically Administered Retargeted Oncolytic Herpes Simplex Viruses-Clearance and Biodistribution in Naïve and HSV-Preimmune Mice. *Cancers (Basel)* 2023;15:4042.
33 Vannini A, Parenti F, Forghieri C, *et al*. Innovative retargeted oncolytic herpesvirus against nectin4-positive cancers. *Front Mol Biosci* 2023;10:1149973.
34 Vannini A, Parenti F, Bressanin D, *et al*. Towards a Precision Medicine Approach and In Situ Vaccination against Prostate Cancer by PSMA-Retargeted oHSV. *Viruses* 2021;13:2085.
35 Gianni T, Leoni V, Sanapo M, *et al*. Genotype of Immunologically Hot or Cold Tumors Determines the Antitumor Immune Response and Efficacy by Fully Virulent Retargeted oHSV. *Viruses* 2021;13:1747.
36 Mineo J-F, Bordron A, Baroncini M, *et al*. Low HER2-expressing glioblastomas are more often secondary to anaplastic transformation of low-grade glioma. *J Neurooncol* 2007;85:281–7.
37 Alessandrini F, Menotti L, Avitabile E, *et al*. Eradication of glioblastoma by immuno-virotherapy with a retargeted oncolytic HSV in a preclinical model. *Oncogene* 2019;38:4467–79.
38 Nguyen KG, Vrabel MR, Mantooth SM, *et al*. Localized Interleukin-12 for Cancer Immunotherapy. *Front Immunol* 2020;11:575597.
39 Reisoli E, Gambini E, Appolloni I, *et al*. Efficacy of HER2 retargeted herpes simplex virus as therapy for high-grade glioma in immunocompetent mice. *Cancer Gene Ther* 2012;19:788–95.
40 Gambini E, Reisoli E, Appolloni I, *et al*. Replication-competent herpes simplex virus retargeted to HER2 as therapy for high-grade glioma. *Mol Ther* 2012;20:994–1001.
41 Alessandrini F, Ceresa D, Appolloni I, *et al*. Glioblastoma models driven by different mutations converge to the proneural subtype. *Cancer Lett* 2020;469:S0304-3835(19)30565-8:447–55:.
42 Menotti L, Avitabile E, Gatta V, *et al*. HSV as A Platform for the Generation of Retargeted, Armed, and Reporter-Expressing Oncolytic Viruses. *Viruses* 2018;10:352.
43 Tierney N, Cook D. Expanding Tidy Data Principles to Facilitate Missing Data Exploration, Visualization and Assessment of Imputations. *J Stat Soft* 2023;105:1–31.
44 Nimmerjahn F, Ravetch JV. Fcgamma receptors as regulators of immune responses. *Nat Rev Immunol* 2008;8:34–47.
45 Voskoboinik I, Whisstock JC, Trapani JA. Perforin and granzymes: function, dysfunction and human pathology. *Nat Rev Immunol* 2015;15:388–400.
46 Balkwill F. Tumour necrosis factor and cancer. *Nat Rev Cancer* 2009;9:361–71.
47 Josephs SF, Ichim TE, Prince SM, *et al*. Unleashing endogenous TNF-alpha as a cancer immunotherapeutic. *J Transl Med* 2018;16:242.
48 Kane A, Yang I. Interferon-gamma in brain tumor immunotherapy. *Neurosurg Clin N Am* 2010;21:77–86.
49 Jorgovanovic D, Song M, Wang L, *et al*. Roles of IFN-γ in tumor progression and regression: a review. *Biomark Res* 2020;8:49.
50 Shalhout SZ, Miller DM, Emerick KS, *et al*. Therapy with oncolytic viruses: progress and challenges. *Nat Rev Clin Oncol* 2023;20:160–77.